

## Supporting Information

### Seamless polymer solar cell module architecture built upon self-aligned alternating interfacial layers

#### 5 Experimental

*Device Fabrication:* The module cells were fabricated with a conjugated polymer of poly[N-9-heptadecanyl-2,7-carbazole-alt-5,5-(4,7-di-2-thienyl-2,1,3-benzothiadiazole)] (PCDTBT) blended with the fullerene derivative [6,6]-phenyl C70-butyric acid methyl ester (PC<sub>70</sub>BM). The conjugated polymer of PCDTBT was synthesized and used. PC<sub>70</sub>BM and polyethyleneimine (PEI) were purchased and used without additional purification. The patterned ITO substrates were cleaned and ultrasonicated in deionized water, acetone and isopropyl alcohol, in sequence, dried in a drying-oven overnight. A 0.5 wt% solution containing the PEI in water was spin-cast with the thickness of approximately 2 nm at 5,000 rpm for 30 s and then dried at 80°C for 10 min in the atmosphere. The MoO<sub>x</sub> films with the thickness of 15 nm were deposited on a half region of the ITO/PEI layer by thermal evaporation under a pressure of  $<10^{-7}$  Torr and at an evaporation rate of 0.2 Å/s. A 0.4 wt% solution containing the mixture of PCDTBT:PC<sub>70</sub>BM (1:4) in dichlorobenzene was spin-cast onto the dual charge-collecting layers, followed by annealing at 80°C for 10 min in dry nitrogen atmosphere to form a thin film with the thickness of approximately 70 nm. The top MoO<sub>x</sub> layer with the thickness of 15 nm was then post-evaporated onto the rest half-area of the underlying ITO/PEI regions on the active layer. The cell fabrication was finalized by the thermal evaporation of the Al electrodes with the thickness of 100 nm using a shadow mask under a pressure of  $<10^{-7}$  Torr.

*Measurements:* The *J-V* characteristics of the unencapsulated devices were measured in the ambient air using a Keithley 236 Source Measure Unit (SMU), under Air Mass 1.5 global (AM 1.5G) illumination from a calibrated solar simulator with an irradiation intensity of 10, 50 and 100 mW/cm<sup>2</sup> from an Abet Technologies Sun 3000 Solar Simulator. Cross-sectional TEM samples were prepared using focused

ion-beam process. The TEM images and the EDS data were obtained by HRTEM (JEOL JEM-3000) operated at 300 kV. KPFM measurements on the surface of devices were carried out in a dry nitrogen atmosphere to suppress contamination from moisture and oxygen. Frequency modulated KPFM (FM-KPFM) images were obtained using a Pt/Ir coated silicon cantilever tip with a resonance frequency of 5 350 kHz (Nanofocus n-Tracer). The cantilever tip was driven by alternating electrical modulation of 2 kHz with amplitude of 1 Vpp and the sample was grounded.

10

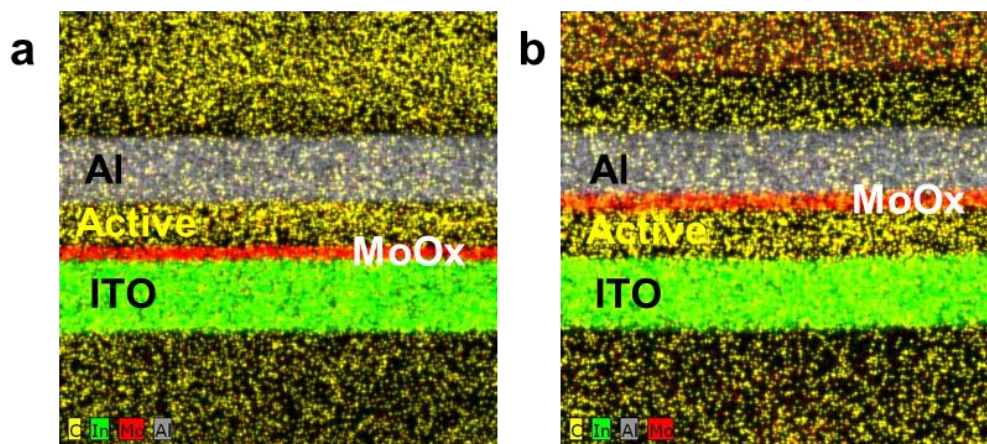


**Figure S1.** The EDS mapping results support the dual subcells with the opposite charge-selecting polarities in (a) the conventional- and (b) the inverted configuration.

15

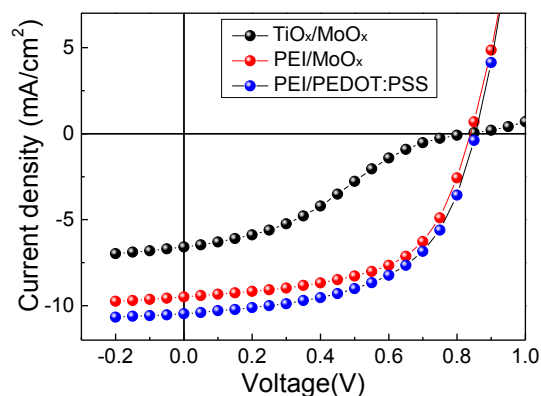
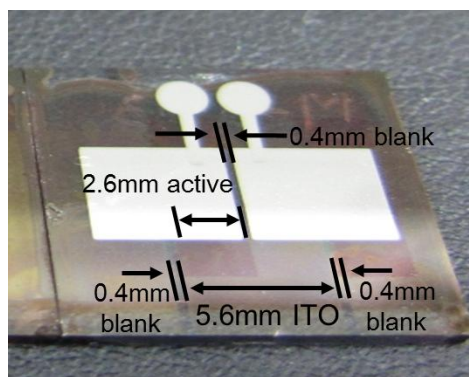


**Figure S2.** Comparison of the photovoltaic performances in the devices with various interfacial layers. The device incorporated with the  $\text{TiO}_x$ - and the PEI layer between the ITO and the  $\text{MoO}_x$  layer shows the anomalous S-shape and the usual  $J$ - $V$  characteristics, respectively. On contrary, the  $\text{MoO}_x$  and the PEDOT:PSS layer are exchangeable with the comparable device performance, respectively. These photovoltaic responses with the different interfacial layers ensure the charge tunnelling through the underlying PEI layer with the various HTL materials.



10

**Figure S3.** Four series connected module cell with SELECT electrodes, where the active width 2.6 mm is defined as the overlapping between the top (Al) and bottom (ITO) electrode and the blank 0.4 mm is defined as the non-overlapping region between the two electrodes. Pads of the top electrode are for characterizing the unit cells.

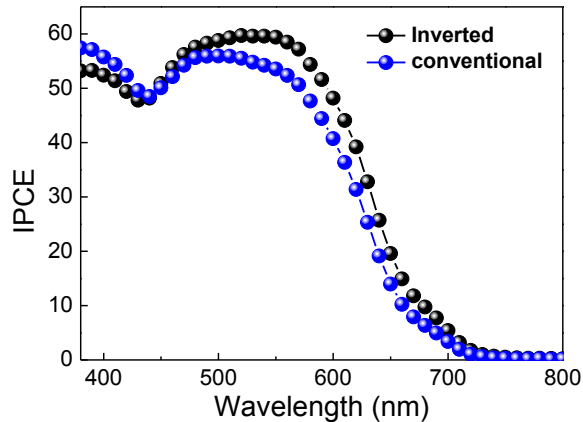


**Figure S4.** The incident photon conversion efficiency (IPCE) spectra measured for the subcells in the 5 conventional- and the inverted device configurations.

10

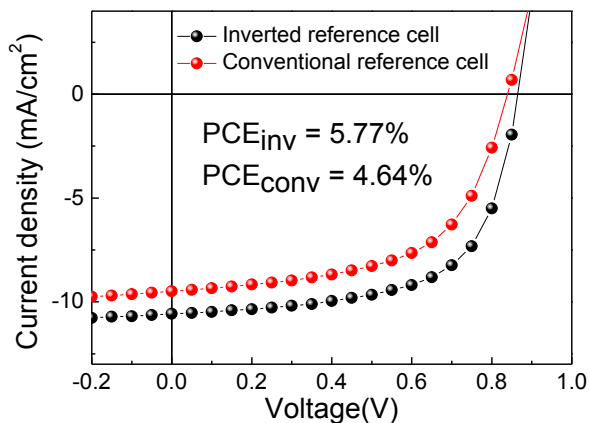


**Figure S5.** The photovoltaic responses of the small-sized reference lab-cells in the different device configurations demonstrate the PCEs of 5.77 and 4.64% for the inverted- and the conventional subcells, respectively.

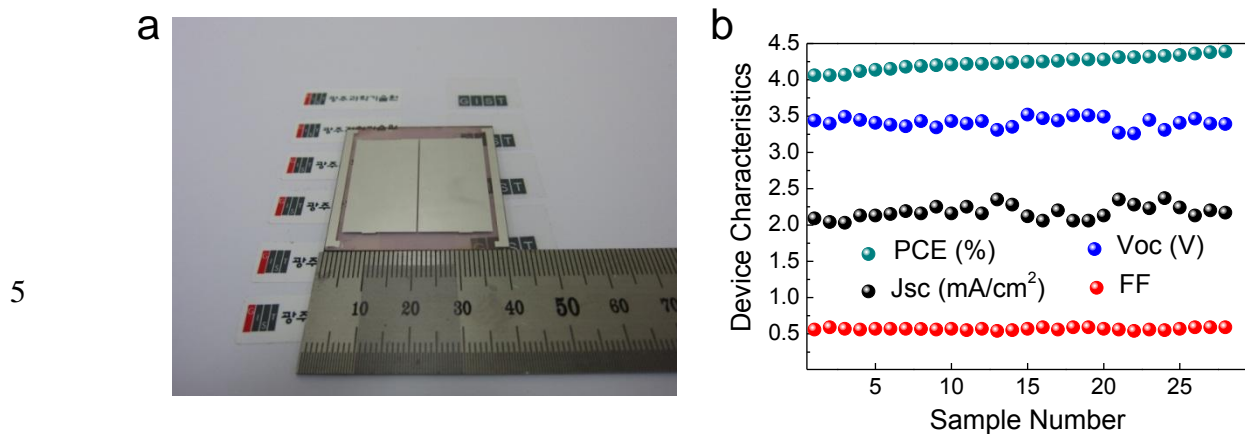
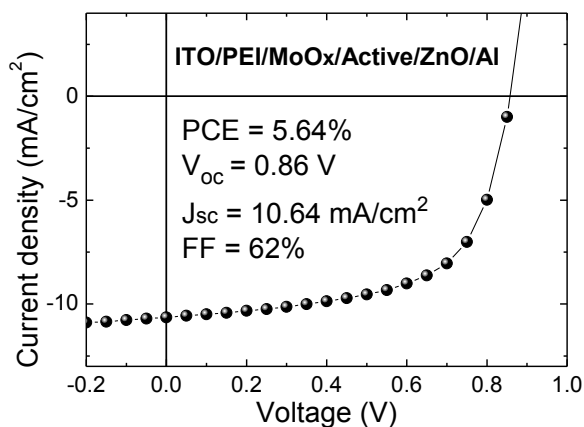


**Figure S6.** (a) A photograph of the module cell with the subcell width of 8.5 mm and the designated 10 illumination area of 1,068 mm<sup>2</sup>. (b) Corresponding characteristics of 28 devices demonstrate the PCEs of 4.39 and 4.24% for the highest attainable and the average value in this module cell architecture, respectively.



15

**Figure S7.** The photovoltaic characteristics of the subcell incorporated with the electron transporting layer of ZnO in the conventional configuration, which yields the PCE of 5.64% comparable to that of the inverted subcell.

**Table S1.** The operational device parameters in the module cell with a subcell width of 2.6 mm.

Parameters	$V_{oc}$ (V)	$J_{sc}$ (mA/cm <sup>2</sup> )	$FF$ (%)	$PCE$ (%)
5				
<b>Subcells (inverted)</b>	0.86	10.25	56	4.94
	0.86	10.12	56	4.87
10 <b>Subcells (conventional)</b>	0.88	9.16	57	4.59
	0.86	8.74	58	4.36
<b>Active area</b>	3.48	2.10	60	4.40
15 <b>Module cell</b>	3.48	1.82	60	3.81

20

**Table S2.** The  $FF$ , the active area efficiency and the module cell efficiency as functions of the subcell width.

25 Subcell width (mm)	$FF$ (%)	active area efficiency (%)	module cell efficiency (%)	geometric fill factor (%)
2.6	60	4.40	3.81	86.6
5.0	59	4.38	4.06	92.6
30 7.5	57	4.38	4.15	94.7
10.0	57	4.34	4.18	96.3
11.3	55	4.19	4.05	96.7

35

**Table S3.** The optimized device parameters and the module cell efficiency as functions of the light intensity.

Light intensity (Sun)	$J_{sc}$ (mA/cm <sup>2</sup> )	$V_{oc}$ (V)	$FF$ (%)	$PCE$ (%)
1.0	2.12	3.52	57	4.24
45 0.5	1.15	3.48	58	4.64
0.1	0.24	3.28	60	4.78